

The Tissue-Specific lncRNA *Fendrr* Is an Essential Regulator of Heart and Body Wall Development in the Mouse

Phillip Grote,¹ Lars Wittler,^{1,5} David Hendrix,^{3,4,5} Frederic Koch,^{1,5} Sandra Währisch,¹ Arica Beisaw,¹ Karol Macura,¹ Gaby Bläss,¹ Manolis Kellis,^{3,4} Martin Werber,¹ and Bernhard G. Herrmann^{1,2,*}

¹Max Planck Institute for Molecular Genetics, Department of Developmental Genetics, Ihnestr. 63-73, 14195 Berlin, Germany

²Charité-University Medicine Berlin, Institute for Medical Genetics-Campus Benjamin Franklin, Hindenburgdamm 30, 12203 Berlin, Germany

³Computer Science and Artificial Intelligence Laboratory, Massachusetts Institute of Technology, Cambridge, MA 02139, USA

⁴Broad Institute of Massachusetts Institute of Technology and Harvard, Cambridge, MA 02142, USA

⁵These authors contributed equally to this work

*Correspondence: herrmann@molgen.mpg.de

<http://dx.doi.org/10.1016/j.devcel.2012.12.012>

SUMMARY

The histone-modifying complexes PRC2 and TrxG/MLL play pivotal roles in determining the activation state of genes controlling pluripotency, lineage commitment, and cell differentiation. Long noncoding RNAs (lncRNAs) can bind to either complex, and some have been shown to act as modulators of PRC2 or TrxG/MLL activity. Here we show that the lateral mesoderm-specific lncRNA *Fendrr* is essential for proper heart and body wall development in the mouse. Embryos lacking *Fendrr* displayed upregulation of several transcription factors controlling lateral plate or cardiac mesoderm differentiation, accompanied by a drastic reduction in PRC2 occupancy along with decreased H3K27 trimethylation and/or an increase in H3K4 trimethylation at their promoters. *Fendrr* binds to both the PRC2 and TrxG/MLL complexes, suggesting that it acts as modulator of chromatin signatures that define gene activity. Thus, we identified an lncRNA that plays an essential role in the regulatory networks controlling the fate of lateral mesoderm derivatives.

INTRODUCTION

Embryonic development commences with the formation of a group of pluripotent stem cells, which give rise to all cell types of the body. Development then proceeds through the coordinated action of cellular proliferation, patterning, lineage commitment, and differentiation, which are controlled by transcriptional regulators acting in a cell type-specific manner. The activity of genes encoding such regulatory proteins depends largely on the chromatin structure at their promoters and the associated regulatory elements. The histone-modifying Polycomb repressive complexes (PRC1/PRC2) and the Trithorax group/MLL protein complexes (TrxG/MLL) play pivotal roles in the control of chromatin structure and, hence, gene activity of a subset of developmentally important regulators (Schuettengruber et al.,

2007). In particular, PRC2 catalyzes the methylation of histone H3 at lysine 27 (H3K27me₃), which is repressive to gene activity, while the TrxG/MLL complex catalyzes the methylation of histone H3 at lysine 4 (H3K4me₃), which acts as an activating mark (Margueron and Reinberg, 2011; Schuettengruber et al., 2011). Thus, PRC2 and TrxG/MLL have opposing activities, and both are essential for embryonic development (O'Carroll et al., 2001; Yu et al., 1995).

It has been shown that components of both the PRC2 and TrxG/MLL complexes are able to interact with long noncoding RNAs (lncRNAs) (Zhao et al., 2008, 2010; Wang et al., 2011). Recent reports have suggested that lncRNAs may target PRC2 or TrxG/MLL to specific genomic loci, and thus contribute to the histone modification status and activity level of target genes (Rinn et al., 2007; Khalil et al., 2009; Bertani et al., 2011; Guttman and Rinn, 2012). In vitro knockdown experiments have revealed the involvement of lncRNAs in gene regulatory networks controlling embryonic stem (ES) cell differentiation (Guttman et al., 2011), and functional studies have provided evidence for the roles of several lncRNAs (Wang et al., 2011; Hu et al., 2011; Kretz et al., 2012; Rinn et al., 2007; Gupta et al., 2010; Ulitsky et al., 2011). For instance, the knockdown of *HOTTIP* by an RCAS-shRNA in the developing chick limb resulted in a shortening of the distal bony elements of the limb, and morpholino-mediated knockdown of *megamind* and *cyrano* in zebrafish embryos revealed important roles for these lncRNAs in organogenesis (Wang et al., 2011; Ulitsky et al., 2011). However, stringent genetic approaches for probing the role of lncRNAs in mouse embryogenesis using loss-of-function analyses have not yet been reported.

Here we have identified an lncRNA, which we have termed *Fendrr*, that is specifically expressed in nascent lateral plate mesoderm. We inactivated *Fendrr* by gene targeting in ES cells and show that *Fendrr* is essential for proper development of tissues derived from lateral mesoderm, specifically the heart and the body wall. We illustrate that *Fendrr* acts by modifying the chromatin signatures of genes involved in the formation and differentiation of the lateral mesoderm lineage through binding to both the PRC2 and TrxG/MLL complexes. Furthermore, we provide evidence that an oligonucleotide corresponding to part of the *Fendrr* transcript can bind to dsDNA in target promoters.

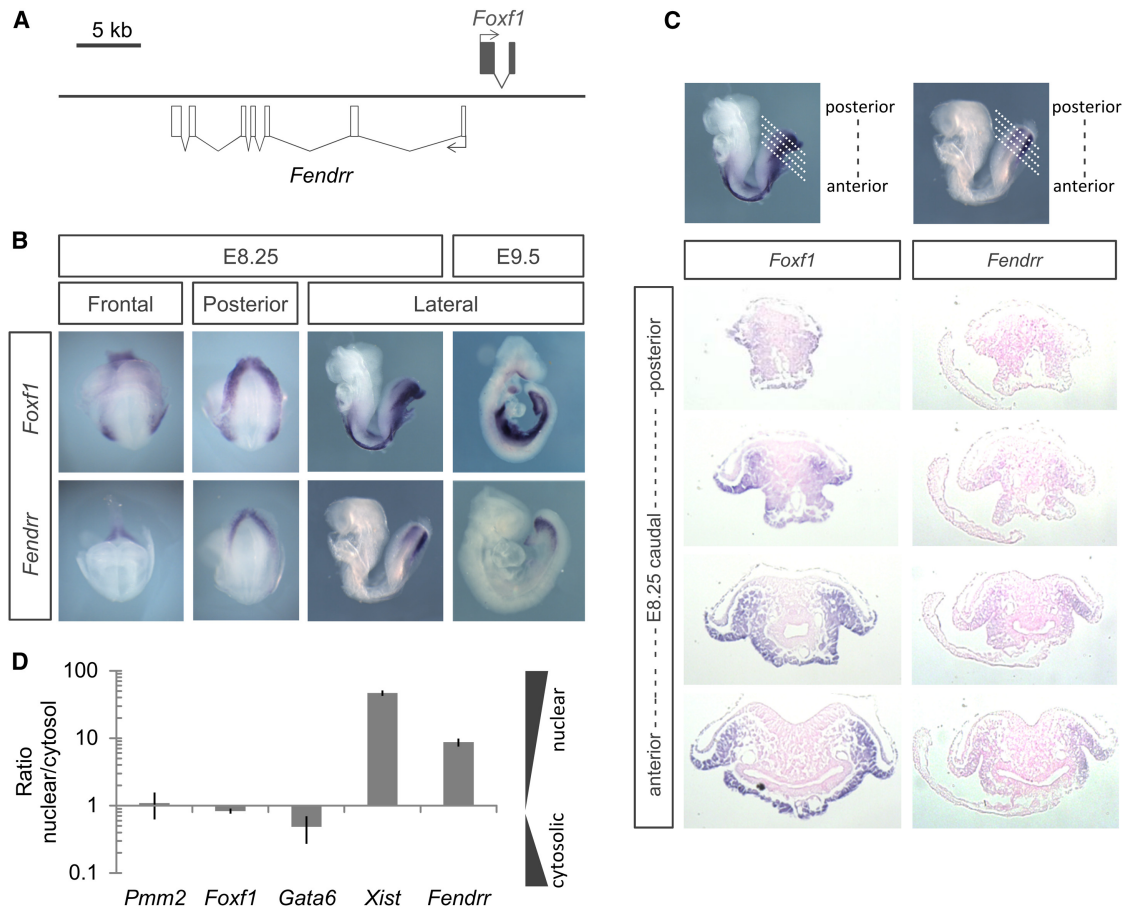


Figure 1. *Fendrr* Is Transiently Expressed in Nascent LPM of Developing Mouse Embryos

(A) Schematic of the genomic region of *Fendrr* and *Foxf1*.

(B) Whole-mount in situ hybridization of mouse embryos at E8.25 and E9.5.

(C) Transverse sections of E8.25 embryos following whole-mount in situ hybridization analysis of *Foxf1* or *Fendrr*.

(D) qPCR analysis of cDNA derived from the cytosolic or nuclear fraction of cells obtained from E9.5 embryo caudal ends; the log₁₀ ratio of nuclear to cytosolic cDNA is presented (n = 3, SD).

RESULTS

Fendrr Expression Is Restricted to Nascent Lateral Plate Mesoderm

We searched for differentially expressed lncRNAs in six different tissues dissected from early somite-stage mouse embryos (TS12, E8.25, three to six somites) using RNA-seq and ChIP-seq analyses. From this data set, we identified a gene that is specifically transcribed in the posterior mesoderm. We isolated it by RACE-PCR from embryonic cDNA and determined its 2,397 base pair (bp) sequence and gene structure (Figure 1A). The gene consists of seven exons and is transcribed divergently from the transcription factor-coding gene *Foxf1*. Its transcriptional start site is located 1,250 bp upstream of the 5'-end of *Foxf1*. We termed this lncRNA *Fendrr* (Fetal-lethal noncoding developmental regulatory RNA).

Whole-mount in situ hybridization showed that *Fendrr* is confined to the caudal end of the lateral plate mesoderm (LPM) of midgestation embryos, which gives rise to ventral structures such as the heart and body wall (Figures 1B and 1C). We could

not detect *Fendrr* expression in other tissues or in organs of later stage embryos using qPCR analysis (data not shown). In the caudal LPM it is coexpressed with *Foxf1*, while in more anterior LPM cells that are undergoing differentiation, *Fendrr* is down-regulated, whereas *Foxf1* expression is maintained in the splanchnic mesoderm (Peterson et al., 1997; Mahlapuu et al., 2001a). Quantitative PCR analysis of RNA extracted from the nuclear or cytosolic fraction of E9.5 caudal end cells showed that *Fendrr* RNA is predominantly localized in the nucleus, consistent with its human ortholog in cultured cells (Figure 1D) (Khalil et al., 2009).

Loss of *Fendrr* Causes Embryonic Lethality

To investigate the function of *Fendrr* in mouse development, we first knocked down *Fendrr* transcripts using a method for shRNAmir-mediated RNA interference in vivo (Vidigal et al., 2010). A reduction in *Fendrr* transcripts to 40% of the wild-type level caused no phenotype (data not shown). Therefore, we consecutively replaced the first exon of *Fendrr* on both chromosomes in ES cells with a strong transcriptional stop signal

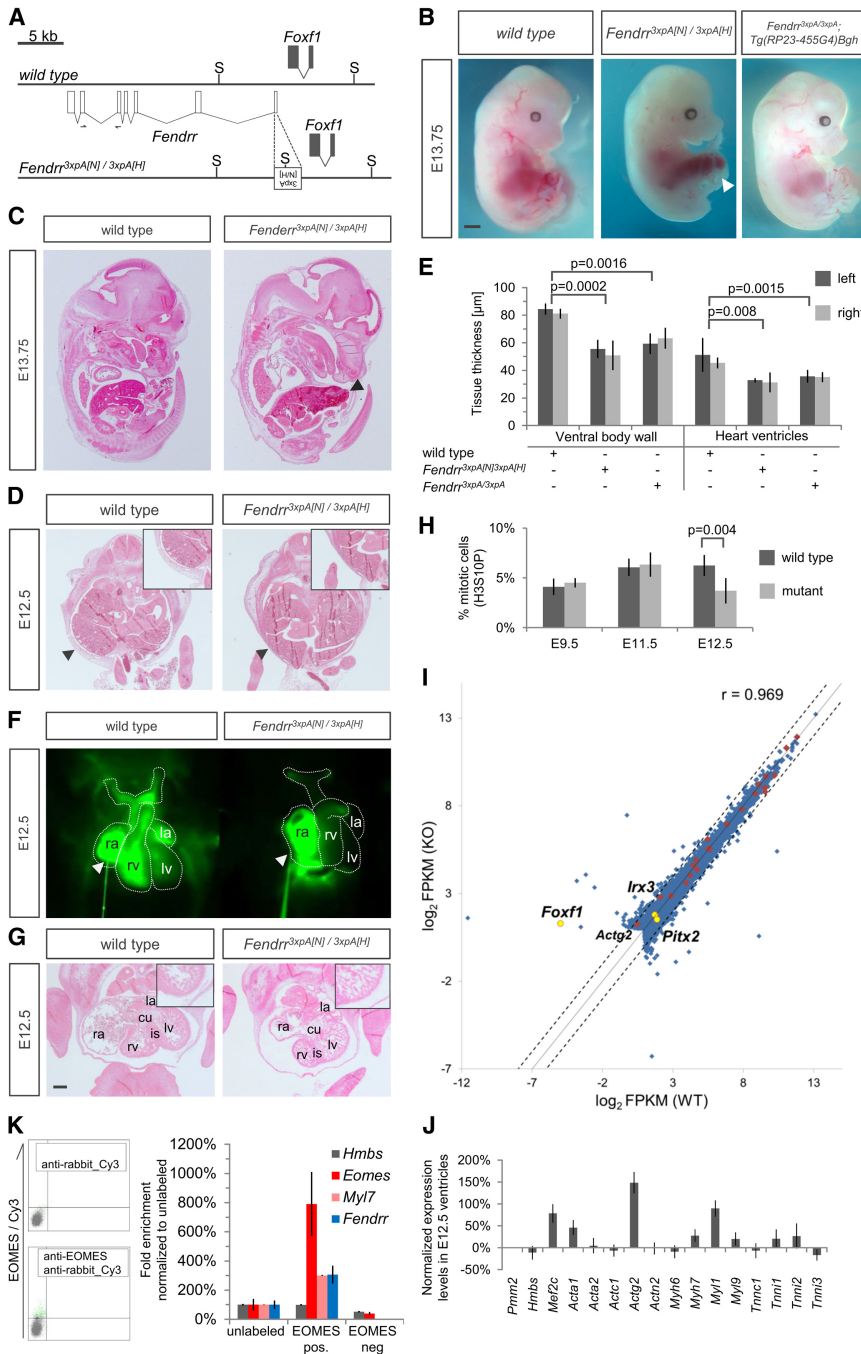


Figure 2. Heart and Body Wall Development Are Impaired in Mutants Lacking *Fendrr* Transcripts

(A) Schematic showing the wild-type (upper) and targeted (lower) *Fendrr-Foxf1* genomic regions; the first exon of *Fendrr* was replaced with a 3xpA stop cassette. Arrows indicate primers for qPCR. (B) E13.75 embryos derived from wild-type or homozygous *Fendrr* mutant ES cells (*Fendrr*^{3xpA[N]/3xpA[H]}), or from mutant cells containing a modified rescue BAC transgene (*Tg(RP23-455G4)Bgh*). The tail and limbs have been removed. Scale bar, 1 mm.

(C) Eosin-stained sagittal sections of E13.75 wild-type and *Fendrr* mutant embryos showing liver protrusion in the latter (arrowhead).

(D and G) Transverse histological sections of E12.5 wild-type and mutant embryos at the midtrunk (D) or chest level (G). rv, right ventricle; is, interventricular septum; cu, atrio-ventricular endocardial cushion; la, left atrium; lv, left ventricle. Scale bar, 200 μm.

(E) Tissue thickness measured from Eosin-stained transverse sections of E12.5 wild-type and homozygous mutant embryos; values from both sides were combined for paired t test analysis. Mean ± SD, (n = 3).

(F) Fluorescent imaging of E12.5 wild-type (n = 3) or mutant (n = 5) embryo hearts injected with FluoSpheres into the right atrium (white arrowhead); images were taken at 75 s of injection (see also Movie S1). ra, right atrium; rv, right ventricle; lv, left ventricle; la, left atrium.

(H) Percentage of mitotic cells (H3S10P) in heart ventricles determined on two distinct sections each of three different embryos. Paired t test analysis and mean ± SD, n = 3.

(I) Scatter plot of transcript abundances (FPKM) derived from RNA-seq analysis of E12.5 mutant compared to wild-type ventricles with one value per gene; genes with an FPKM of less than 2 in both samples were omitted. The dotted lines represent a fold-change of 2 and 0.5. The samples show a high correlation, with a Pearson correlation coefficient of 0.969.

(J) Normalized expression levels of heart genes determined by qPCR analysis of E12.5 mutant

ventricles compared to wild-type (values set to zero; *Pmm2* and *Hmbs* are housekeeping genes); mean ± SD, n = 3.

(K) Gating of EOMES-positive cells from a single cell suspension of E6.5 wild-type embryo proper, and qPCR analysis of RNA derived from EOMES-positive and EOMES-negative cells.

See also Figure S1.

(3xpA) by homologous recombination (Friedrich and Soriano, 1991), thereby generating a *Fendrr* null mutant (Figure 2A). Successful targeting of both alleles in ES cells was confirmed by Southern blot analysis (Figure S1A available online). We confirmed loss of *Fendrr* transcripts in the caudal ends of *Fendrr* null embryos generated by tetraploid complementation

(Gertsenstein, 2011) using whole-mount in situ hybridization (Figure S1B).

Homozygous mutants (*Fendrr*^{3xpA[N]/3xpA[H]}) were found to be embryonic lethal around E13.75 (Figures 2B and S1C). At this stage they appeared pale and displayed a prominent omphalocele, wherein parts of the developing liver and all umbilical

vessels protruded from the ventral body (88.9%, $n = 9$) (Figures 2B and 2C). Omphalocele and embryonic death persisted after removal of the PGK-Neo and PGK-Hygro selection cassettes (genotype *Fendrr*^{3xpA/3xpA}; Figures S1C and S1D).

To rule out that the phenotype of *Fendrr*^{3xpA/3xpA} mutant embryos was due to compromised genetic integrity of the ES cells we performed a rescue experiment. We introduced a BAC clone containing a functional *Fendrr* gene next to an inactivated *Foxf1* locus into *Fendrr*^{3xpA/3xpA} mutant ES cells and generated embryos by tetraploid complementation. These *Fendrr*^{3xpA/3xpA}; *Tg(RP23-455G4)Bgh* embryos showed a normal expression pattern of *Fendrr* at E9.5 (Figure S1B) and expressed approximately half of the wild-type level of *Fendrr* RNA, as expected from a single functional allele (Figure S1E). The *Foxf1* expression level was unchanged in rescued embryos in E9.5 caudal ends as compared to wild-type embryos (Figure S1F). They appeared phenotypically normal until E17.5, while at E18.5 rescue was observed in the majority of embryos (Figures 2B, S1C, and S1G). Thus, the embryonic rescue confirmed the genetic integrity of the mutant ES cells used in the following experiments, and we conclude that the lethal phenotype of *Fendrr*^{3xpA[N]/3xpA[H]} and *Fendrr*^{3xpA/3xpA} embryos is entirely due to loss of *Fendrr* transcripts.

To determine the etiology of the mutant phenotype, we examined the morphology of embryos at stage E12.5, when mutants still appeared phenotypically normal. Measurements of the thickness of the ventral body wall, a derivative of the somatic LPM lineage, showed a severe reduction in homozygous mutant as compared to wild-type embryos (Figures 2D and 2E; $n = 3$). This suggests a possible cause for the observed omphalocele: that the weak body wall of the mutant is insufficient to resist the pressure from the growing liver (Figures 2B and 2C).

Besides an omphalocele, mutant embryos also displayed blood accumulation in the right heart chamber (Figure S1H). To assess functioning of the heart, which is a derivative of the splanchnic LPM lineage, we incubated E12.5 embryos at 37°C, injected FluoSpheres into the right atrium of the beating heart, and followed the blood circulation with time-lapse imaging (see Experimental Procedures). In wild-type embryos, we observed dispersion of the fluorescence through the right ventricle and into the arteries, while in *Fendrr* mutants the fluorescence accumulated in the right atrium (Figure 2F; Movie S1). This indicated that the heart function of mutant embryos is impaired, providing a plausible explanation for embryonic death observed around E13.5.

To gain further insight into the cellular basis of this heart malfunction, we performed histological analyses of E12.5 mutant hearts. Heart sections revealed hypoplasia of the myocardium in the mutants, affecting the ventricular walls and interventricular septum (Figure 2G). Measurements of the thickness of the ventricular walls revealed a severe reduction in mutant as compared to wild-type hearts (Figure 2E). To examine the cellular basis for the hypoplasia, we counted the mitotic cells on sections of wild-type and mutant hearts at three developmental stages. No difference was found at E9.5 and E11.5, whereas E12.5 mutant hearts showed a marked decrease of mitotic cells (Figure 2H). We detected no significant apoptosis in E12.5 wild-type or mutant hearts by cleaved caspase-3 (Asp175) staining on sections (data not shown). These data indicate that the

cardiac hypoplasia in mutants may be due to impaired proliferation of cardiac myocytes at later stages of heart development.

To investigate the changes in gene expression related to the heart phenotype on a genome-wide scale, we analyzed the transcriptomes of E12.5 wild-type and *Fendrr* mutant hearts by RNA-seq. We found no strong changes in the expression levels of any of the known heart control genes, nor of genes associated with cell proliferation control in mutant tissue (Figure 2I). Quantitative PCR analysis of a subset of heart-specific structural genes confirmed the RNA-seq data (Figures 2J and 2I) (Lin et al., 1997; Olson, 2006). Thus, the transcriptome data did not offer a molecular explanation for the heart phenotype of the *Fendrr* mutant.

The combined data show that *Fendrr* mutants exhibit myocardial dysfunction, which most likely is the cause of embryonic death. Moreover, the impaired development of both the heart and the body wall illustrates that loss of *Fendrr* transcripts in nascent LPM causes impaired development of derivatives of both the somatic and splanchnic LPM lineages.

Loss of *Fendrr* Affects the Epigenetic Modification and Expression of Factors Controlling Lateral Mesoderm Differentiation

Cardiac mesoderm derives from the first lateral mesoderm formed in the primitive streak at the early to midstreak stage (E6.5-7). To ensure that *Fendrr* is expressed in the prospective cardiac mesoderm at this early embryonic stage, we isolated *Eomes* expressing cells from E6.5 mouse embryos by fluorescence activated cell sorting using an EOMES-specific antibody (Figure 2K). *Eomes* and *Myf7* are markers of the early cardiac mesoderm lineage (Costello et al., 2011). We determined the RNA expression level of *Eomes*, *Myf7*, and *Fendrr* in EOMES-positive and EOMES-negative cells in comparison to unlabeled control cells. We found coexpression of *Myf7* and *Fendrr* exclusively in EOMES-positive cells, while neither transcript was detectable in EOMES-negative cells (Figure 2K). Thus, *Fendrr* is indeed expressed in cardiac mesoderm progenitor cells. Because formation of the heart tube occurs around E8.0, we asked whether the expression of four important regulators of heart development, *Gata4*, *Gata6*, *Tbx5*, and *Nkx2-5* were affected at this stage (Olson, 2006; Watanabe and Buckingham, 2010). We found that *Gata6* and *Nkx2-5* expression in the heart field of E8.5 mutant embryos was significantly increased in comparison to wild-type tissue, while *Gata4* and *Tbx5* remain unchanged (Figure 3A).

Next, we asked whether these changes in gene expression were mirrored by alterations of the histone methylation status at the promoters of these genes. The histone methyltransferase complexes TrxG/MLL and PRC2 deposit activating H3K4me3 and repressive H3K27me3 marks, respectively, and both complexes have been shown to be involved in lineage commitment in vitro (Margueron and Reinberg, 2011; Surface et al., 2010; Schuettengruber et al., 2011). We found no significant change in the status of H3K27me3 at the promoters of the heart control genes analyzed, while the H3K4me3 mark of the *Gata6* and *Nkx2-5*, but not *Gata4* or *Tbx5* promoters was increased (Figure 3B). Thus, loss of *Fendrr* results in an increase of H3K4 trimethylation in a subset of heart control gene promoters, mirrored by an increased expression of these genes.

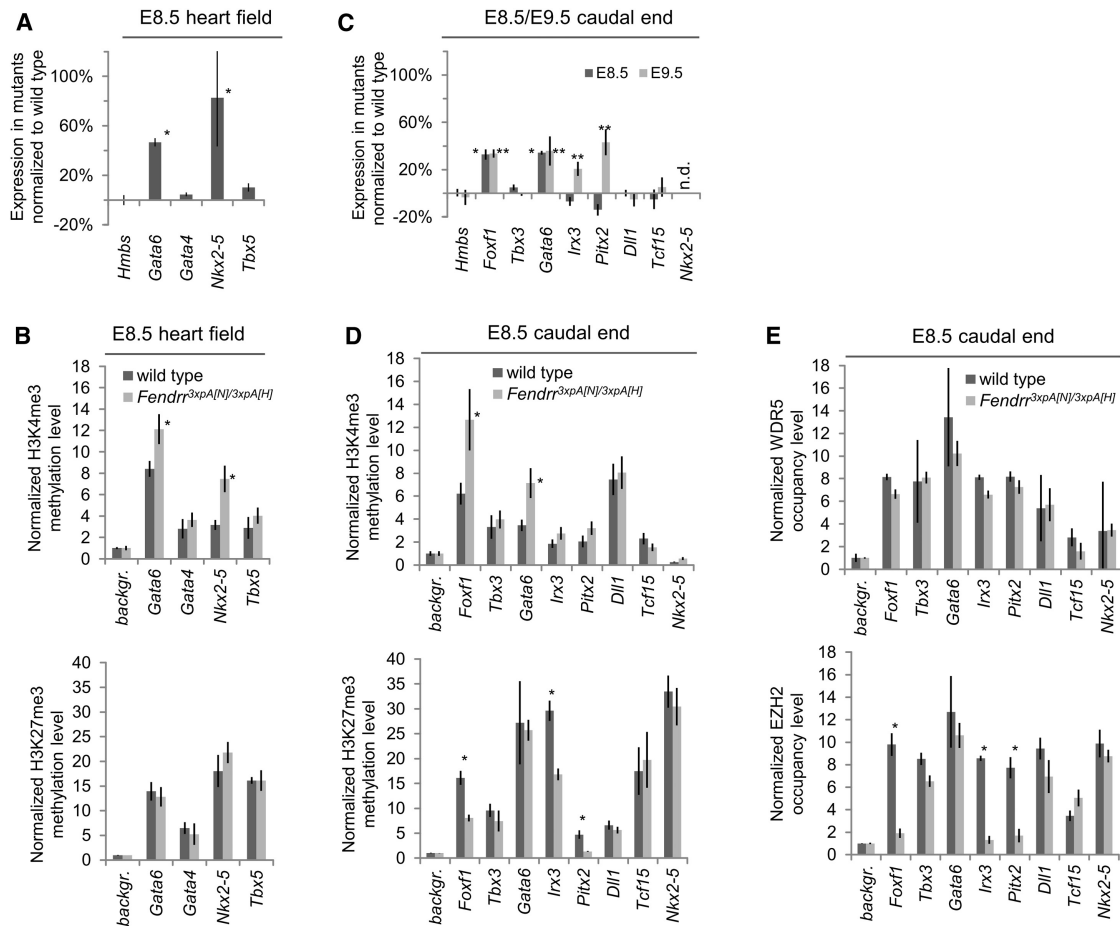


Figure 3. Loss of *Fendrr* Affects Epigenetic Promoter Modification and Expression of Transcriptional Regulators in E8.5 Embryonic Hearts and Caudal Ends

(A and C) Normalized expression levels of transcriptional regulators in heart fields (A) and caudal ends (C) of *Fendrr* mutant embryos compared to wild-type controls. n.d., not detectable; * $p \leq 0.02$ in E8.5, ** $p \leq 0.05$ in E9.5.

(B and D) Quantitative comparison of the levels of activating H3K4me3 (* $p \leq 0.03$) and repressive H3K27me3 (* $p \leq 0.05$) methylation marks in the promoters of control genes in E8.5 heart fields (B) and caudal ends (D) from *Fendrr* mutant and wild-type embryos.

(E) Quantitative comparison of the levels of WDR5 or EZH2 (* $p \leq 0.05$) bound to promoters. All measurements were performed by qPCR. Means \pm SD, $n = 3$ for expression and $n = 2$ for ChIP analysis.

See also Figure S2.

Because *Gata6* is widely expressed in the LPM, including nascent LPM and heart progenitor cells, we wanted to determine whether changes in *Gata6* expression and promoter histone modifications were already present in nascent LPM. In addition, we analyzed the expression of the LPM control genes *Foxf1*, *Pitx2*, and *Irx3*, which play important roles in determining the splanchnic and somatic LPM lineages, along with *Tbx3* (Mahlapuu et al., 2001b; Rallis et al., 2005; Kitamura et al., 1999). The presomitic mesoderm (PSM) marker genes *Dll1* and *Tcf15* were included as controls.

The expression levels of *Gata6* and *Foxf1* were significantly increased in the caudal ends of E8.5 mutant embryos, while *Irx3*, *Tbx3*, and the PSM marker genes were not affected at this stage (Figure 3C). This increase in *Gata6* and *Foxf1* expression persisted in the nascent LPM of E9.5 mutant embryos. In addition, *Irx3* and *Pitx2* expression was also increased at this later stage, during which the progenitors of the ventral body wall are gener-

ated (Figure 3C). The expression of *Foxc2*, *Foxl1*, and *Mthfsd*, located in close vicinity to *Foxf1* and *Fendrr*, was unchanged, excluding unspecific effects of *Fendrr* gene locus alterations on neighboring genes in the knockout allele (Figure S2A).

Similarly to what was observed in the heart, changes in gene expression were accompanied by changes in the methylation status of the promoters. The *Gata6* and *Foxf1* promoters of mutant E8.5 embryos showed a strong increase in H3K4me3, and the *Irx3* and *Pitx2* promoters a slight increase in H3K4me3 (Figure 3D). In contrast to *Gata6*, which showed no difference in the repressive mark, the H3K27me3 levels at the *Foxf1*, *Irx3*, and *Pitx2* promoters of mutant embryos were strongly reduced as compared to wild-type (Figure 3D). The methylation status of the control PSM marker gene promoters was not altered for either the H3K4me3 or the H3K27me3 marks.

Next we asked whether the changes in histone modifications observed correlated with altered occupancy of the PRC2

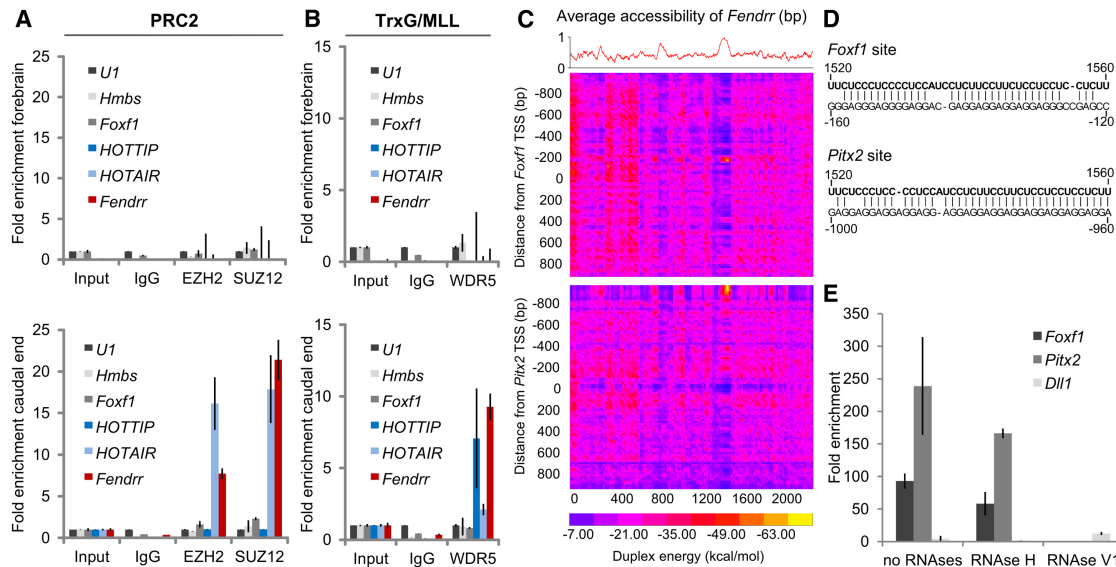


Figure 4. *Fendrr* Binds to the PRC2 and TrxG/MLL Complexes and to Target Promoters

(A and B) RNA coimmunoprecipitation (RIP) from forebrain (upper panels) and caudal end (lower panels) lysates from wild-type embryos using antibodies directed against EZH2 and SUZ12 (A) or WDR5 (B); normal rabbit IgG was used as control. Fold enrichment has been normalized to nonenriched input sample and U1 rRNA. *Foxf1* and *Hmbs* RNA served as negative control. Mean \pm SD are shown ($n = 3$).

(C) Binding potential between *Fendrr* and genomic regions. The red curve shows the average probability of single-stranded RNA (Ding et al., 2004). The heat map represents the base-pairing energy for an RNA/RNA duplex model for 40-bp regions along the *Fendrr* transcript and 2,000 bp around the TSS of *Foxf1* (top) and *Pitx2* (bottom).

(D) Representation of the predicted interaction of the *Fendrr* RNA region and the promoter DNA region exhibiting the lowest free energy of approximately -70 kcal/mol (see yellow spot in C).

(E) In vitro RNA/dsDNA binding assay utilizing biotin tagged RNA oligos as bait. Bars represent normalized enrichment of indicated 2,000-bp promoter fragment over background using a control RNA oligonucleotide (Mean \pm SD, $n = 3$).

See also Figure S3.

and/or TrxG/MLL complexes at the respective promoters. We analyzed the presence of PRC2 or TrxG/MLL by ChIP with antibodies against EZH2, SUZ12 (PRC2 components), or WDR5 (TrxG/MLL component), followed by qPCR analysis of the promoter regions. Immunoprecipitation of the *Foxf1*, *Irx3*, and *Pitx2* promoter regions with EZH2 or SUZ12 antibodies from mutant caudal end tissue was drastically reduced compared to wild-type tissue, whereas all other promoters were not affected (Figures 3E and S2B). In contrast, promoter occupancy of WDR5 in caudal end tissue was unchanged for all of the promoters tested (Figure 3E). In addition, no changes in EZH2, SUZ12, or WDR5 occupancy were observed in heart tissue for any of the promoters tested (Figure S2C).

These combined data show that *Fendrr* has differential effects on the histone modification of promoters for transcriptional regulators in the lateral mesoderm and at least one of its derivatives, the cardiac mesoderm. The data suggest that the primary role of *Fendrr* is to promote occupancy of the PRC2 complex on particular promoters for LPM control genes, resulting in an increase of the repressive H3K27me3 mark, accompanied by a reduction in gene expression. In addition, probably via a different mechanism, *Fendrr* is involved in controlling the level of the activating H3K4me3 mark on a subset of promoters, thereby modifying the expression level of those genes.

We asked if the epigenetic changes caused by loss of *Fendrr* at the *Foxf1*, *Pitx2*, and *Irx3* promoters, which caused upregula-

tion of these genes in lateral mesoderm, had an effect on the expression of these genes in E12.5 cardiac tissue. RNA-seq data showed a moderate, ectopic expression of *Foxf1* in E12.5 mutant hearts, whereas no *Foxf1* transcripts were detected in wild-type tissue (Figure 2). *Irx3* and *Pitx2* expression, which is active in the wild-type E12.5 heart, was not altered in the mutant organ. These data suggest that the epigenetic changes caused by *Fendrr* at its target promoters in lateral mesoderm may persist through consecutive stages of differentiation and thus also take effect in the descendants of the cells exposed to *Fendrr* activity.

***Fendrr* Binds In Vivo to the PRC2 and TrxG/MLL Histone-Modifying Complexes**

The ChIP data prompted us to investigate whether *Fendrr* interacts directly with the PRC2 and/or TrxG/MLL complexes in mouse embryos. We immunoprecipitated the PRC2 complex with specific antibodies directed against EZH2 or SUZ12 from lysates of wild-type E9.5 embryonic caudal ends, which express *Fendrr*, and from forebrains, which are devoid of *Fendrr* transcripts. Coprecipitated RNA was extracted and quantified by qPCR. The lncRNA *HOTAIR* served as positive control (Tsai et al., 2010). *Fendrr* and *HOTAIR* transcripts were coprecipitated with both PRC2 components from the caudal end tissue where they are expressed, but not from forebrain (Figure 4A). These data demonstrate that *Fendrr* transcripts bind to PRC2

in the mouse embryo, confirming data previously obtained in cultured human foreskin fibroblasts for the human orthologous lncRNA (Khalil et al., 2009). Next, we tested whether *Fendrr* transcripts could interact with the TrxG/MLL component WDR5. The lncRNA *HOTTIP* served as positive control (Wang et al., 2011). Again, both *Fendrr* and *HOTTIP* transcripts were coimmunoprecipitated with WDR5 from the caudal end, but not from forebrain tissue (Figure 4B). In contrast, *Fendrr* RNA was not coprecipitated with the PRC1 component RING1B, the NuRD complex component LSD1, or SIRT6 (Figure S3A). Thus, *Fendrr* RNA binds to PRC2 and TrxG/MLL and discriminates between various histone-modifying complexes.

Fendrr Binds to the *Foxf1* and *Pitx2* Promoters In Vitro

Because *Fendrr* binds to the PRC2 complex and loss of *Fendrr* resulted in a strong reduction of PRC2 occupancy at the *Foxf1*, *Pitx2*, and *Irx3* promoters, we asked whether *Fendrr* is able to bind directly to any of these promoters. We calculated the binding potential of *Fendrr* to fragments covering 1 kb upstream to 1 kb downstream of the transcriptional start site of each of the three genes. The heat map revealed a short stretch in the *Fendrr* RNA predicted to bind to a complementary region in the *Foxf1* and *Pitx2* promoters (Figures 4C and 4D). The *Irx3* promoter was negative within the region analyzed, just as the promoters of *Dll1* and *Tcf15*, which served as negative controls (Figure S3B). We used a synthetic RNA oligonucleotide coupled to psoralen and biotin at either end and performed an in vitro binding assay (Besch et al., 2004; Schmitz et al., 2010). The promoter fragments of both *Foxf1* and *Pitx2*, but not of *Dll1*, coprecipitated with this RNA oligomer (Figure 4E). Coprecipitation occurred in the presence of RNaseH, but was prevented by RNaseV1 treatment. The former enzyme specifically cuts RNA in DNA/RNA heteroduplexes, while the latter cleaves base-paired nucleotides. The data show that *Fendrr* can bind to double-stranded *Foxf1* and *Pitx2* promoter fragments, and suggest triplex formation at the complementary region (Buske et al., 2012). The data in combination with findings discussed above confirm that *Fendrr* acts in *cis* (at the *Foxf1*) and in *trans* (at the *Pitx2* and possibly other promoters).

The combined data suggest that *Fendrr* anchors PRC2 at its target promoters, thereby increasing PRC2 occupancy and H3K27 trimethylation, which consequently leads to attenuation of target gene expression. Moreover, the coexpression of the transcriptional regulator *Foxf1* and the lncRNA *Fendrr* in lateral mesoderm links the transcriptional regulatory network with the epigenetic regulatory network acting in this tissue.

DISCUSSION

Fendrr is a regulatory RNA, which mediates the modification of the epigenetic landscape of target promoters thereby causing attenuation of the expression of transcription factors that are important in lateral mesoderm differentiation.

Our data suggest that changes in epigenetic modifications within promoters of genes involved in a gene regulatory network (GRN) can cause deleterious effects, which are similar to those seen following the loss of a single crucial transcription factor. For instance, *Foxf1* is essential for the separation of splanchnic and somatic mesoderm (Mahlapuu et al., 2001b), where it is

required to inhibit *Irx3* expression in the splanchnic mesoderm and direct it to the somatic mesoderm lineage (Mahlapuu et al., 2001b). *Pitx2* is required for heart and ventral body wall development (Kitamura et al., 1999). However, at this point we cannot conclude that the mutant phenotype observed is indeed caused by increased expression of several transcriptional regulators, nor can we exclude that failure of *Fendrr* binding to TrxG/MLL at presently unidentified promoters leading to downregulation of target genes may contribute to the mutant phenotype.

Compound heterozygosity of *Gata4* and *Gata6* has been shown to result in embryonic lethality demonstrating that a threshold of both genes is required to support cardiovascular development (Xin et al., 2006). Moreover, heterozygosity for *Foxf1* or *Pitx2* results in haplo-insufficiency phenotypes, indicating that a threshold level of each of these regulators is critical for proper embryonic development (Mahlapuu et al., 2001a; Liu et al., 2003). While on the basis of current knowledge this is well conceivable, it is harder to envisage how an excess of transcriptional regulators might perturb embryonic processes.

An important feature of *Fendrr* is its long-term effect. In general, the action of transcription factors is restricted to the cells in which they are expressed. In contrast, the epigenetic signatures of regulatory elements set early in a differentiation process can persist through several stages of differentiation. The ectopic upregulation of *Foxf1* in E12.5 *Fendrr* mutant hearts indicates that *Fendrr* is involved in epigenetic modifications affecting activation or repression of its target genes in descendants of the cells in which *Fendrr* was, but no longer is, active. Thus, disturbances in the epigenetic prepatterning within the early precursor cells of organs and tissues may have far-reaching consequences on subsequent cell proliferation, patterning or differentiation processes in the descendants of those cells. Cardiac myocyte proliferation in *Fendrr* mutant hearts is not affected before E12.5, 6 days after *Fendrr* expression in the cardiac progenitor cells of the lateral mesoderm has been lacking. Future work has to address how this late effect in cardiac tissue is triggered by *Fendrr* loss in cardiac progenitor cells.

The gene pairing of *Fendrr* and *Foxf1* highlights the intriguing transcriptional and functional coupling of a divergent lncRNA with an adjacent regulatory protein, both of which are essential for development of the same embryonic tissue. Such lncRNA: protein-coding gene neighbors are found throughout the genome (Cabili et al., 2011) and this functional link may reveal a more general mechanism for the control of patterning and lineage commitment (Cabili et al., 2011; Ulitsky et al., 2011; Margueron and Reinberg, 2011; Ørom et al., 2010).

EXPERIMENTAL PROCEDURES

Fluorescent Imaging

All animal procedures were conducted as approved by the local authorities (LAGeSo Berlin) under the license number G0368/08. Embryos were dissected at E12.5 into warm M2 medium, and kept at 37°C. Embryos were fixed onto temperature-adjusted SYLGARD 184 Silicone Elastomer mounting plates using needles to expose their thoraxes. Sonicated FluoSpheres (20 nm, Life Technologies) were diluted 1:10 with PBS and injected into the right atrium using a glass microcapillary for 10 s with mild pressure. Hearts were imaged under a Leica MZ 16FA microscope equipped with a GFP3 filter and videos recorded using the Leica LAS AF software.

RNA Coimmunoprecipitation

RNA coimmunoprecipitation was carried out as previously described (Galgano et al., 2008). Magnetic Protein A and G beads (Life Technologies) were used for isolation of antibody-bound protein/RNA complexes. Coprecipitated RNA was reverse transcribed using random hexamers, and cDNA content quantified by qPCR. Antibodies used were anti-EZH2 (Active Motif), anti-SUZ12 (Abcam), anti-WDR5 (Bethyl Laboratories, Inc.), anti-RING1B (Active Motif), anti-LSD1 (Abcam), and anti-SIRT6 (Abcam). For oligonucleotide sequences, see the Supplemental Experimental Procedures (Zhao et al., 2008).

Binding Potential Calculations and RNA/dsDNA Interaction Assay

The average probability of single-stranded RNA was computed by *sfold* with a length parameter of 200 and $W = 1$ (Ding et al., 2004). Base-pairing energy for an RNA/RNA duplex model for 40-bp regions along the *Fendrr* transcript and 2,000 bp around the TSS of *Foxf1* and *Pitx2* was calculated (Lorenz et al., 2011). The duplex energy is computed for each such region, staggered by 20 bp, and displayed in a heatmap. Probabilities are then averaged for a sliding window of 40 bp to give the average RNA accessibility of the region that is binding.

The RNA/DNA interaction assay was essentially carried out as described (Besch et al., 2004). Briefly, 1 pmol of promoter fragment (−1 kb to +1 kb from the transcriptional start site) were incubated at 37°C for 30 min with 100 pmol of PsoralenC6-UCCCCUCCAUCCUCUUCUCCUCCUCCU CUUCUUU-BiotinTEG (*Fendrr*) or unspecific PsoralenC6-UCCCCUGUGGG UGGGGUGGGGGUCUUU-BiotinTEG RNA oligonucleotides (Biomers) (Schmitz et al., 2010). The reaction was UV (265 nm) treated as described. Preblocked M270 Streptavidin beads (Life Technologies) were used to precipitate bound DNA in the presence or absence of RNase H or V1. Fold enrichment was determined by the ratio of specific to unspecific DNA precipitate obtained from three replicates.

ACCESSION NUMBERS

The GenBank accession number for the *Fendrr* full-length cDNA sequence reported in this paper is JQ973641. The GEO accession number for the RNA-seq data reported in this paper is GSE43078.

SUPPLEMENTAL INFORMATION

Supplemental Information includes three figures, one movie, and Supplemental Experimental Procedures and can be found with this article online at <http://dx.doi.org/10.1016/j.devcel.2012.12.012>.

ACKNOWLEDGMENTS

We thank Silke Sperling and Cornelia Dorn for discussion on the heart phenotype and qPCR primers for heart marker analysis; Marc Sultan, Alexander Kovacsovics, and Matthias Linser for RNA sequencing; members of the animal facility for breeding of mice and strain maintenance; and Tracie Pennimpe for comments on the manuscript. We are grateful to Mikhail Sukchev for providing the modified RP23-455G4 BAC.

Received: April 24, 2012

Revised: December 19, 2012

Accepted: December 20, 2012

Published: January 28, 2013

REFERENCES

Bertani, S., Sauer, S., Bolotin, E., and Sauer, F. (2011). The noncoding RNA *Mistral* activates *Hoxa6* and *Hoxa7* expression and stem cell differentiation by recruiting MLL1 to chromatin. *Mol. Cell* 43, 1040–1046.

Besch, R., Giovannangeli, C., Schuh, T., Kammerbauer, C., and Degitz, K. (2004). Characterization and quantification of triple helix formation in chromosomal DNA. *J. Mol. Biol.* 341, 979–989.

Buske, F.A., Bauer, D.C., Mattick, J.S., and Bailey, T.L. (2012). Triplexator: detecting nucleic acid triple helices in genomic and transcriptomic data. *Genome Res.* 22, 1372–1381.

Cabilli, M.N., Trapnell, C., Goff, L., Koziol, M., Tazon-vega, B., Regev, A., and Rinn, J.L. (2011). Integrative annotation of human large intergenic noncoding RNAs reveals global properties and specific subclasses. *Genes Dev.* 25, 1–13.

Costello, I., Pimeisl, I.-M., Dräger, S., Bikoff, E.K., Robertson, E.J., and Arnold, S.J. (2011). The T-box transcription factor *Eomesodermin* acts upstream of *Mesp1* to specify cardiac mesoderm during mouse gastrulation. *Nat Cell Biol.* 13, 1084–1091.

Ding, Y., Chan, C.Y., and Lawrence, C.E. (2004). *Sfold* web server for statistical folding and rational design of nucleic acids. *Nucleic Acids Res.* 32(Web Server issue), W135–41.

Friedrich, G., and Soriano, P. (1991). Promoter traps in embryonic stem cells: a genetic screen to identify and mutate developmental genes in mice. *Genes Dev.* 5, 1513–1523.

Galgano, A., Forrer, M., Jaskiewicz, L., Kanitz, A., Zavolan, M., and Gerber, A.P. (2008). Comparative analysis of mRNA targets for human PUF-family proteins suggests extensive interaction with the miRNA regulatory system. *PLoS ONE* 3, e3164.

Gertsenstein, M. (2011). Tetraploid Complementation Assay, S. Pease and T.L. Saunders, eds. (Berlin: Springer Berlin Heidelberg).

Gupta, R.A., Shah, N., Wang, K.C., Kim, J., Horlings, H.M., Wong, D.J., Tsai, M.C., Hung, T., Argani, P., Rinn, J.L., et al. (2010). Long non-coding RNA *HOTAIR* reprograms chromatin state to promote cancer metastasis. *Nature* 464, 1071–1076.

Guttman, M., and Rinn, J.L. (2012). Modular regulatory principles of large non-coding RNAs. *Nature* 482, 339–346.

Guttman, M., Donaghey, J., Carey, B.W., Garber, M., Grenier, J.K., Munson, G., Young, G., Lucas, A.B., Ach, R., Bruhn, L., et al. (2011). lincRNAs act in the circuitry controlling pluripotency and differentiation. *Nature* 477, 295–300.

Hu, W., Yuan, B., Flygare, J., and Lodish, H.F. (2011). Long noncoding RNA-mediated anti-apoptotic activity in murine erythroid terminal differentiation. *Genes Dev.* 25, 2573–2578.

Khalil, A.M., Guttman, M., Huarte, M., Garber, M., Raj, A., Rivea Morales, D., Thomas, K., Presser, A., Bernstein, B.E., van Oudenaarden, A., et al. (2009). Many human large intergenic noncoding RNAs associate with chromatin-modifying complexes and affect gene expression. *Proc. Natl. Acad. Sci. USA* 106, 11667–11672.

Kitamura, K., Miura, H., Miyagawa-Tomita, S., Yanazawa, M., Katoh-Fukui, Y., Suzuki, R., Ohuchi, H., Suehiro, A., Motegi, Y., Nakahara, Y., et al. (1999). Mouse *Pitx2* deficiency leads to anomalies of the ventral body wall, heart, extra- and periocular mesoderm and right pulmonary isomerism. *Development* 126, 5749–5758.

Kretz, M., Webster, D.E., Flockhart, R.J., Lee, C.S., Zehnder, A., Lopez-Pajares, V., Qu, K., Zheng, G.X., Chow, J., Kim, G.E., et al. (2012). Suppression of progenitor differentiation requires the long noncoding RNA *ANCR*. *Genes Dev.* 26, 338–343.

Lin, Q., Schwarz, J., Bucana, C., and Olson, E.N. (1997). Control of mouse cardiac morphogenesis and myogenesis by transcription factor *MEF2C*. *Science* 276, 1404–1407.

Liu, W., Selever, J., Lu, M.-F., and Martin, J.F. (2003). Genetic dissection of *Pitx2* in craniofacial development uncovers new functions in branchial arch morphogenesis, late aspects of tooth morphogenesis and cell migration. *Development* 130, 6375–6385.

Lorenz, R., Bernhart, S.H., Höner Zu Siederdisen, C., Tafer, H., Flamm, C., Stadler, P.F., and Hofacker, I.L. (2011). *ViennaRNA Package 2.0*. *Algorithms Mol. Biol.* 6, 6.

Mahlapuu, M., Enerbäck, S., and Carlsson, P. (2001a). Haploinsufficiency of the forkhead gene *Foxf1*, a target for sonic hedgehog signaling, causes lung and foregut malformations. *Development* 128, 2397–2406.

Mahlapuu, M., Ormestad, M., Enerbäck, S., and Carlsson, P. (2001b). The forkhead transcription factor *Foxf1* is required for differentiation of extra-embryonic and lateral plate mesoderm. *Development* 128, 155–166.

- Margueron, R., and Reinberg, D. (2011). The Polycomb complex PRC2 and its mark in life. *Nature* 469, 343–349.
- Olson, E.N. (2006). Gene regulatory networks in the evolution and development of the heart. *Science* 313, 1922–1927.
- O'Carroll, D., Erhardt, S., Pagani, M., Barton, S.C., Surani, M.A., and Jenuwein, T. (2001). The polycomb-group gene *Ezh2* is required for early mouse development. *Mol. Cell. Biol.* 21, 4330–4336.
- Peterson, R.S., Lim, L., Ye, H., Zhou, H., Overdier, D.G., and Costa, R.H. (1997). The winged helix transcriptional activator HFH-8 is expressed in the mesoderm of the primitive streak stage of mouse embryos and its cellular derivatives. *Mech. Dev.* 69, 53–69.
- Rallis, C., DeI Buono, J., and Logan, M.P.O. (2005). *Tbx3* can alter limb position along the rostrocaudal axis of the developing embryo. *Development* 132, 1961–1970.
- Rinn, J.L., Kertesz, M., Wang, J.K., Squazzo, S.L., Xu, X., Bruggmann, S.A., Goodnough, L.H., Helms, J.A., Farnham, P.J., Segal, E., and Chang, H.Y. (2007). Functional demarcation of active and silent chromatin domains in human HOX loci by noncoding RNAs. *Cell* 129, 1311–1323.
- Schmitz, K.M., Mayer, C., Postepska, A., and Grummt, I. (2010). Interaction of noncoding RNA with the rDNA promoter mediates recruitment of DNMT3b and silencing of rRNA genes. *Genes Dev.* 24, 2264–2269.
- Schuettengruber, B., Chourrout, D., Vervoort, M., Leblanc, B., and Cavalli, G. (2007). Genome regulation by polycomb and trithorax proteins. *Cell* 128, 735–745.
- Schuettengruber, B., Martinez, A.-M., Iovino, N., and Cavalli, G. (2011). Trithorax group proteins: switching genes on and keeping them active. *Nat. Rev. Mol. Cell Biol.* 12, 799–814.
- Surface, L.E., Thornton, S.R., and Boyer, L.A. (2010). Polycomb group proteins set the stage for early lineage commitment. *Cell Stem Cell* 7, 288–298.
- Tsai, M.-C., Manor, O., Wan, Y., Mosammamaparast, N., Wang, J.K., Lan, F., Shi, Y., Segal, E., and Chang, H.Y. (2010). Long noncoding RNA as modular scaffold of histone modification complexes. *Science* 329, 689–693.
- Ulitsky, I., Shkumatava, A., Jan, C.H., Sive, H., and Bartel, D.P. (2011). Conserved function of lincRNAs in vertebrate embryonic development despite rapid sequence evolution. *Cell* 147, 1537–1550.
- Vidigal, J.A., Morkel, M., Wittler, L., Brouwer-Lehmitz, A., Grote, P., Macura, K., and Herrmann, B.G. (2010). An inducible RNA interference system for the functional dissection of mouse embryogenesis. *Nucleic Acids Res.* 38, e122.
- Wang, K.C., Yang, Y.W., Liu, B., Sanyal, A., Corces-Zimmerman, R., Chen, Y., Lajoie, B.R., Protacio, A., Flynn, R.A., Gupta, R.A., et al. (2011). A long noncoding RNA maintains active chromatin to coordinate homeotic gene expression. *Nature* 472, 120–124.
- Watanabe, Y., and Buckingham, M. (2010). The formation of the embryonic mouse heart: heart fields and myocardial cell lineages. *Ann. N Y Acad. Sci.* 1188, 15–24.
- Xin, M., Davis, C.A., Molkenin, J.D., Lien, C.L., Duncan, S.A., Richardson, J.A., and Olson, E.N. (2006). A threshold of GATA4 and GATA6 expression is required for cardiovascular development. *Proc. Natl. Acad. Sci. USA* 103, 11189–11194.
- Yu, B.D., Hess, J.L., Horning, S.E., Brown, G.A., and Korsmeyer, S.J. (1995). Altered Hox expression and segmental identity in *Mil*-mutant mice. *Nature* 378, 505–508.
- Zhao, J., Sun, B.K., Erwin, J.A., Song, J.J., and Lee, J.T. (2008). Polycomb proteins targeted by a short repeat RNA to the mouse X chromosome. *Science* 322, 750–756.
- Zhao, J., Ohsumi, T.K., Kung, J.T., Ogawa, Y., Grau, D.J., Sarma, K., Song, J.J., Kingston, R.E., Borowsky, M., and Lee, J.T. (2010). Genome-wide identification of polycomb-associated RNAs by RIP-seq. *Mol. Cell* 40, 939–953.
- Ørom, U.A., Derrien, T., Beringer, M., Gumireddy, K., Gardini, A., Bussotti, G., Lai, F., Zytynicki, M., Notredame, C., Huang, Q., et al. (2010). Long noncoding RNAs with enhancer-like function in human cells. *Cell* 143, 46–58.